ELSEVIER

Journal of Nuclear Materials 258–263 (1998) 1572–1576

journal of nuclear materials

Swelling behaviour and TEM studies of SiC_f/SiC composites after fusion relevant helium implantation

H.W. Scholz [a,1], A.J. Frias Rebelo [a,*], D.G. Rickerby [a], P. Krogul [b], W.E. Lee [b], J.H. Evans [c], P. Fenici [a]

[a] *European Commission, J.R.C., Institute for Advanced Materials, TP 202, 21020 Ispra (VA), Italy*
[b] *Department of Engineering Materials, University of Sheffield, Sheffield, UK*
[c] *Department of Physics, University of London, London, UK*

Abstract

Helium implantation was carried out on SiC_f/SiC (CVI) composites up to doses of 2500 appm, at temperatures of 1175 ± 50 K. In this paper the swelling behaviour of the implanted bending bars is reported. A significant differential swelling effect after the α-implantation was evidenced by the matrix jutting out with respect to the fibre ends, at the side surfaces of the implanted zone. A similar fibre shrinkage together with slight expansion of the matrix was already reported for neutron irradiated materials. However, after α-implantation this effect is enhanced by an increased swelling of the β-SiC matrix. These data are discussed in relation to microstructural observations by Transmission Electron Microscopy.

1. Introduction

SiC-based ceramic matrix composites, when used in commercial fusion reactors as a main structural material near the plasma will form around 2000 appm He per MWa/m^2 due to transmutation reactions [1,2]. Understanding the microstructural mechanisms of degradation caused by this helium in SiC_f/SiC is crucial for any substantial further improvement of this composite in view of applications in fusion technology. This paper deals with swelling results and TEM analysis of Si–C–O fibre based SiC-matrix composites after fusion relevant α-implantation fluences. This experimental approach of irradiation remains only a limited simulation in comparison to the synergetic effects when neutron displacement damage and transmutation reactions will take place in a fusion reactor material. However, the findings from the microstructural deterioration, especially differential swelling, after α-implantation may help future development of SiC_f/SiC for fusion technological use.

2. Experimental

The 2D-SiC_f/SiC_{CVI} composites (Cerasep™ by SEP, France) considered here are made from cross-woven laminates of fibre yarns, the latter containing ~220 filaments (Nicalon™ Si–C–O-fibre NL-202 by Nippon Carbon, Japan). A 0.1 μm thick carbon layer was deposited by CVD onto the fibres prior to Chemical Vapour Infiltration (CVI) of β-SiC as a matrix. Bending specimens with dimensions of $60 \times 8 \times 1.2$ mm^3 were supplied, each containing five stacked layers. The fibre content of the composite was 28 ± 3 vol%. The CVI process leads to a morphology which follows the 2D yarn configuration and inter-bundle pores of ≈300 μm are present, common to this type of SiC matrix processing.

High-fluence helium implantation up to 2500 appm was carried out at the M40 Cyclotron of IAM Ispra. Implanted volume zones extending $4.0 \times 8 \times 0.6$ mm^3 were obtained, located in the centre of the specimen length and ranging through half of its thickness. This

* Corresponding author. Tel.: +39 332 789768; fax: +39 332 789 434; e-mail: artur.rebelo@jrc.it.

[1] Present address: Institute for Ceramics in Mechanical Engineering, Central Laboratory, University of Karlsruhe, Germany.

0022-3115/98/$19.00
PII: S0022-3115(98)00221-9

permitted post-irradiation three-point bending tests with the α-implanted zone under maximum tensile load. Homogeneity of the implantation over the specimen depth was achieved by the 39 MeV α-beam crossing a degrader wheel with 50 pure Al-foils of different thickness before reaching the samples. Lateral homogeneity was attained by wobbling the beam. A helium gas jet blowing directly onto the implanted zone provided target cooling. Controlling the helium flow and pressure in the implantation chamber, the pyrometrically controlled irradiation temperature was kept at 1173 ± 50 K. A concomitant displacement damage of 0.4 ± 0.1 dpa was calculated using the TRIM-code [3] accounting for displacement energies given in [4]. Further implantation details were given in [5].

Sample thickness was measured against the level of a precision table by means of fixed concentricity micrometer gauge, before and after the α-implantation. Fifteen discrete points of touching measurement, equidistantly distributed along the length and broadness of the samples were obtained. Additionally, samples were flipped on the precision table and effective height values over this level were obtained for both sides of the bars. This permitted a differential evaluation of the bending or buckling effects in the implanted samples, which arose in the swollen, implanted front side zone, which expanded against the non-implanted, non-swollen backside. A precision calliper (5 μm sensitivity) was used to evaluate length and broadness in three points each. It featured flat touch-tip surfaces ($\varnothing = 0.5$ mm), so that the local topography of the composite surfaces did not influence the results. Length and broadness measurements error was 10 μm mainly due to tilting, whilst for the thickness the error was limited to 5 μm.

The material was investigated by Scanning Electron Microscopy (SEM). Additionally, helium implanted 2D-SiC_f/SiC_{CVI} were investigated by Transmission Electron Microscopy (TEM), obtaining samples from implanted and not implanted regions for comparison. The x–z plane of the bars was considered, perpendicular to the longitudinal direction of the fibres. Standard ceramographic grinding and polishing techniques were used, followed by dimpling and ion thinning in a GATAN PIPS unit operating at 5.5 kV. TEM samples were examined on a JEOL JEM200CX operating at 200 kV.

3. Results

Swelling and bending of the central length part of the bars was shown to be implantation induced, because as received they were originally flat, with a parallelism tolerance of $\leqslant 20$ μm. The implanted central part of the 2D-SiC_f/SiC_{CVI}-specimens may be seen like a bimetallic strip, where the expansion of one layer causes bending. The 28 mm long wing-zones left and right of the implanted zone resulted to be straight. From the profilometry results, a total deflection δ_α was calculated, which formed within the implanted length section $L_{imp} = 4$ mm. Introducing an implantation induced bending moment M_α:

$$\delta_\alpha = \frac{M_\alpha L_{Imp}^2}{8 E_x I_\alpha},$$

where the moment of inertia $I_\alpha = B_\alpha H_\alpha^3/12$ must be calculated from the swollen geometry. For the total clearance Δ_α of the arcing specimen holds:

$$\Delta_\alpha = \delta_\alpha + \frac{L - L_{Imp}}{2} \sin(\varphi_\alpha),$$

where φ_α is the step angle, which forms at the ends of L_{Imp} as well as between the outer specimen ends and the measurement table. φ_α proved to be symmetrical on the left and right side of the implanted zone. Δ_α resulted from the described height step profilometry. For pure bending holds:

$$\varphi_\alpha = \frac{M_\alpha L_{Imp}}{2 E_x I_\alpha}.$$

From this we have the following:

$$\frac{M_\alpha L_{Imp}^2}{8 E_x I_\alpha} = \Delta_\alpha - \left(\frac{L - L_{Imp}}{2}\right) \sin\left(\frac{M_\alpha L_{Imp}}{2 E_x I_\alpha}\right).$$

Numerical solutions for M_α using measured Δ_α could be found. The maximum *apparent* swelling induced strain $\varepsilon_{x,\alpha,max}$ at the surface of the implanted zone of the specimen in the direction of the length co-ordinate x was:

$$\varepsilon_{x,\alpha,max} = \frac{M_\alpha H_\alpha}{2 E_x I_\alpha}.$$

The maximum uncertainty of this $\varepsilon_{x,\alpha,max}$ is only ±0.02%-points of the strain. Further, H_α and the swollen broadness B_α were measured in the centre of the α-implanted zone L_{Imp}, and were regarded as representative for the whole implanted zone, in order to avoid the influence of swelling constraints from the not implanted specimen zones left and right of the implanted zone on the interpretation. It followed $\varepsilon_{y,\alpha} = (B_\alpha - B)/B$; the maximum relative error of $\varepsilon_{y,\alpha}$ from measurement uncertainties was ±0.25%-points. Moreover, $\varepsilon_{z,\alpha} = (H_\alpha - H)/\langle R_\alpha \rangle_{max}$, where $\langle R_\alpha \rangle_{max}$ is the mean range of the implantation at maximum α-particle energy. Here, the error from measurement uncertainties is as high as ±1.7%-points, because the measured total thickness is very small. The relative volume swelling results:

$$(V_\alpha - V_{Imp})/V_{Imp} = (1 + \varepsilon_{x,\alpha})(1 + \varepsilon_{y,\alpha})(1 + \varepsilon_{z,\alpha}) - 1.$$

The error of the term $(V_\alpha - V_{Imp})/V_{Imp}$ due to measurement uncertainties follows by error propagation to be ±2%-points of the swelling. Table 1 gives the relative swelling for each specific co-ordinate direction of the implantation. Note, that sample Pos.-No. 5 (with

Table 1
Overview on macroscopic swelling of 2D-SiC_f/SiC_{CVI} bend bars after α-implantation; the values added with the ± mark show absolute uncertainties of the measurement, given in %-points of the swelling-strain

Sample SEP	Swelling in the implanted volume zone:					Implanted α-dose	Max. temp.-peak
	Length *apparent* $\varepsilon_{x,\alpha}$ [%]	Length $\varepsilon_{x,\alpha}$ acc. to [6] [%]	Broadness $\varepsilon_{y,\alpha}$ [%]	Thickness $\varepsilon_{z,\alpha}$ [%]	Volume $\frac{V_\alpha - V_{imp}}{V_{imp}}$ [%]	[appm]	[K]
3	0.26 ± 0.02	0.35	0.5 ± 0.25	1.4 ± 1.7	2.2 ± 2.0	2797	1248
4	0.27 ± 0.02	0.36	0.4 ± 0.25	3.6 ± 1.8	4.3 ± 2.1	2738	1302
5	0.15 ± 0.02	0.20	0.0 ± 0.25	3.1 ± 1.8	3.2 ± 2.1	1466	1164
6	0.30 ± 0.02	0.40	0.4 ± 0.25	2.7 ± 1.8	3.4 ± 2.1	2590	1233
7	0.00 ± 0.02	0.00	0.1 ± 0.25	0.6 ± 1.7	0.6 ± 2.0	13	1241
8	0.28 ± 0.02	0.32	0.3 ± 0.25	4.2 ± 1.8	4.8 ± 2.1	2454	1222

reduced α-dose) and Pos.-No. 7 (practically no α-Dose, but typical implantation conditions for some minutes) show the phenomenon of the implantation induced bending to a lesser extent and $\varepsilon_{x,\alpha,max}$ appears to be dependent on the α-dose. Jung et al. [6] also implanted ceramic bending bars partially in a front layer which was representing only a part of the total bar thickness. They also used the implantation induced bending to evaluate the swelling of the bars in the longitudinal direction by analytical approximations which were verified by FEM calculations. Their approach has the advantage to take the Poisson's ratio of the composite into account and to purify the swelling result in the longitudinal direction of swell-bended bars from the back-bending moment of the non-implanted side. Using a Poisson's ratio of $\mu = 0.12$ and the expression for $\varepsilon_{x,\alpha,max}$ in [6] gave results by $\frac{1}{3}$ higher.

SEM examination of side surfaces after α-implantation revealed the matrix to jut out beyond the fibre ends (Fig. 1) by at least twice its diameter on both sides of the 8 mm broad specimen. This is qualitatively known from neutron irradiated 2D-SiC_f/SiC_{CVI}. Quantitative interpretation of this visible feature of differential swelling is however rather difficult, as the woven fibre architecture does not guarantee a precise length difference between the matrix and the fibre-bundle to be evaluated. TEM studies of the matrix phase in the implanted region did not evidence the presence of helium bubbles. The only discerned difference relies on the presence of SiC grains exhibiting black/white contrast, which may indicate the presence of irradiation-induced dislocation loops (Fig. 2(A) and (B)). The fibres, however, are showing up similar features as those observed for the non-implanted

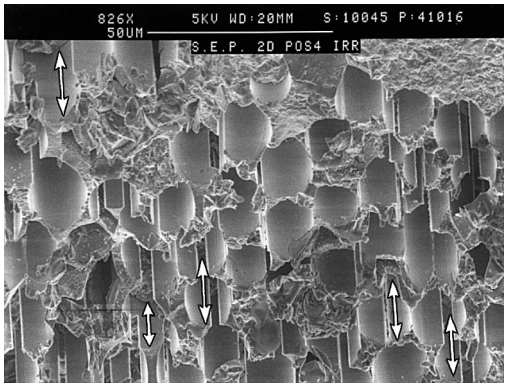

Fig. 1. SEM image of a 2500 appm helium implanted SiC/SiC composite – Lateral Surface.

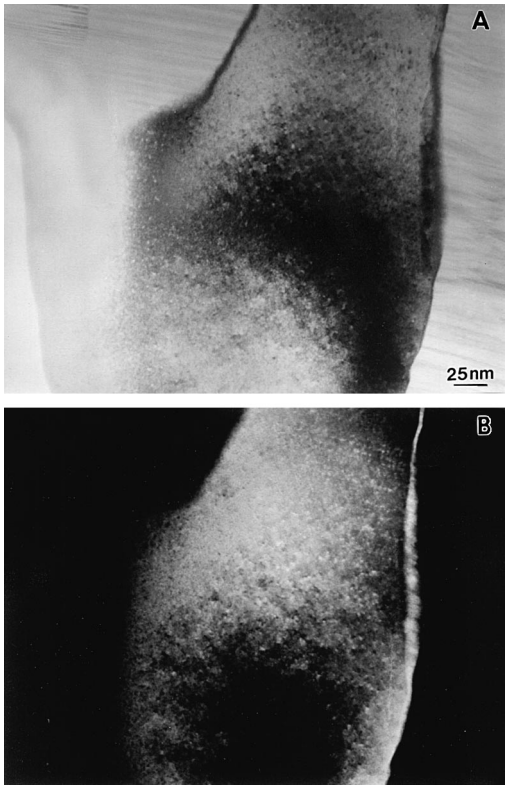

Fig. 2. TEM image of SiC crystal from the matrix composites: (a) bright field; (b) dark field. Black/white contrast evidence of irradiation-induced dislocation loops.

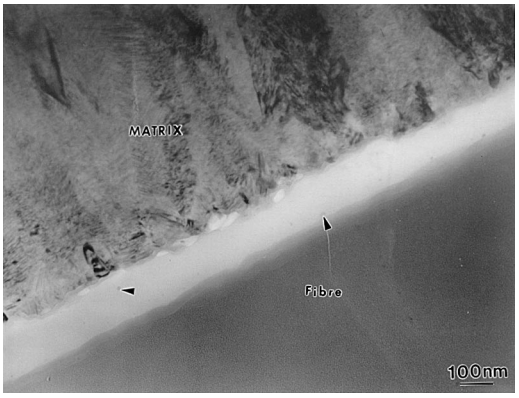

Fig. 3. TEM image of non-implanted zone of SiC/SiC composite – Interface.

regions: small (2 nm) SiC crystallites are surrounded by an amorphous phase that corresponds to the silicon oxycarbide phase characteristic for Si–C–O fibres. Near the carbon layer at the fibre/matrix interface, however, bright voids are visible next to the columnar SiC matrix grains, which are always of rounded shape (Fig. 3). For comparison, these voids are not appearing at the interfaces in the non-implanted zones (Fig. 4). Again in the implanted zone, occasional small (2–5 nm) crystallites are visible within the carbon interface-layer (see arrows in Fig. 3).

4. Discussion

Other possible causes of the swelling were checked by plotting the results in Table 1 versus (1) the geometrical density values of the samples before implantation; (2) the number of ion-beam interruptions which lead to a thermal shocks of the samples in the helium cooling-gas jet; and (3) the maximum temperature peaks of the implantation temperature due to so-called *ion-burst*-phenomena of the α-beam of the cyclotron. However, no influence, neither quantitatively nor qualitatively, of these parameters on the swelling behaviour of the 2D-SiC_f/SiC_{CVI} was found.

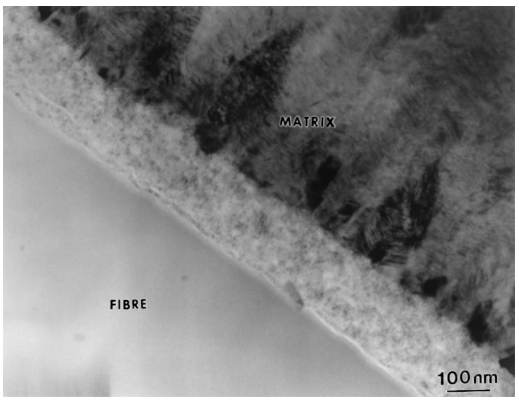

Fig. 4. TEM image of a fibre/matrix interface within the α-implanted zone in SiC/SiC. Voids are visible next to the dense β-SiC matrix grains of the matrix. Arrowed are small crystallites within the interfacial carbon.

Given the substantial difference in helium mobility between the β-SiC of the matrix, the turbostratic carbon interface layer and the nanocrystalline/amorphous phase of the fibres, the possibilities for helium outgassing should be different in these composite constituents as well. Considering the implantation temperature of 1173 K, it is feasible, that the implanted helium was able to outgas from the fibres and their carbon layers, but not from within the polycrystalline matrix. The latter was already shown for monocrystalline, α-SiC by Sasaki et al. [7], who observed helium outgassing from 773 K onward, the first peak, however, at temperatures by 500 K higher than the one used here for implantation. Even at 2073 K, still 85% of the helium was trapped. These experimental findings were also used by Allen [8] to interpret his results on helium lattice locations in α-SiC, emphasising the low vacancy mobility up to 1473 K following from the absence of helium bubbles after annealing at that temperature. Allen concluded on the strong defect trapping by his ion channelling analysis, stating the high possibility of the helium remaining on lattice sites of the SiC crystal. It may be reasonable to transfer these findings to the interpretation, that helium is trapped similarly in the dense, polycrystalline β-SiC of the matrix of 2D-SiC_f/SiC_{CVI}. This, however, would account for the pinpointing of vacancies in the temperature range given here, i.e. a relevant one for a fusion reactor first wall according to the ARIES I reactor study [9]. In fact, the results on geometrical swelling indicate a much higher swelling than the one predicted by only regarding the displacement damage of ~0.4 dpa. Whilst neutron irradiation of both, α-SiC and β-SiC around 1173 K results in rather low linear swelling of ~0.15% due to recombination and probably the annihilation of smallest interstitial defect clusters [2], here the most precise result on $\varepsilon_{x,\alpha,\max}$ indicated helium induced linear swelling of up to ~0.4%. This result is confirmed regarding the specimen broadness swelling $\varepsilon_{y,\alpha,\max}$, for which by the orthotropic nature of the composite similar values were to be expected. Whether in the thickness direction a special mechanism is even further enhancing the swelling $\varepsilon_{z,\alpha,\max}$, cannot be concluded, as the measurement precision was not sufficient and artificial effects like local buckling of matrix infiltrated bundles under compression or even delamination between woven fibre yarn layers may have influenced the results. The evolution of 2D-SiC_f/SiC_{CVI} under irradiation is also featuring fibre densification according to the literature, especially when Si–C–O fibres are employed. This starts at relatively low fluence values [10] and may further

explain the pronounced jutting out effect of the matrix beyond the fibre ends as found on the implanted side surfaces. The small crystallites within the implanted carbon layers forming the fibre/matrix interface may originate from chemical evolution of the fibres, but do not seem to jeopardise the structural integrity of the composite significantly.

5. Conclusions

Differential swelling is observed after homogeneous α-implantation of fusion reactor first wall relevant helium doses into 2D-SiC_f/SiC_{CVI}. At reactor relevant temperatures of 1173 K, comparison with the literature suggests a different swelling regime in the dense matrix SiC than the one known for neutron irradiated SiC, when helium atoms are present. It was speculated, that helium is inhibiting the recombinatorial defect annealing at this temperature level.

In cohesion with the interpretation above, voids were found at non-debonded fibre/matrix interfaces next to the matrix. If these voids are to be interpreted as helium agglomerations, a possible explanation would be the blocking effect of the matrix with respect to the helium diffusing from the partially amorphous fibres and the turbostratic carbon interfaces.

Acknowledgements

The authors thank M. Della Rossa, IAM of JRC Ispra, for the SEM-micrograph. Research grants of the European Commission (“HC&M” program) and the Portuguese Science and Technology Ministry (“PRAXIS XXI” program) provided the financial support for A.J.F.R.

References

[1] L.A. El-Guebaly, Fusion Eng. Des. 28 (1995) 658.
[2] H.W. Scholz, Ph.D. Thesis, University of Karlsruhe, Germany, 1997, Report EUR 17681 DE.
[3] J.P. Biersack, L.G. Haggmark, Nucl. Instr. Meth., 174 (1980) 257.
[4] A. El-Azab, N.M. Ghoniem, J. Nucl. Mater. 191–194 (1992) 92.
[5] H.W. Scholz, A. Frias Rebelo, Thin SiC_f/SiC bending specimens for high fluence helium implantation, in: P. Jung, H. Ullmaier (Eds.), Miniaturised Specimens for Testing of Irradiated Materials, Forschungszentrum Jülich GmbH, Germany, 1995, p. 201.
[6] P. Jung, Z. Zhu, J. Chen, in: Workshop on Defect Production, Accumulation and Material Performance on Irradiation Environments, Davos, Switzerland, 1997, to be published.
[7] K. Sasaki, T. Yano, T. Murayama, T. Iseki, J. Nucl. Mater. 179–181 (1991) 407.
[8] W.R. Allen, J. Nucl. Mater. 210 (1994) 318.
[9] S. Sharafat, N.M. Ghoniem, L.Y. Yee and the ARIES Team, in: Proceedings of Thirteenth Symposium on Fusion Engineering, Knoxville, Tennessee, USA, 2–6 October 1989.
[10] R.J. Jones, L.L. Snead, A. Koyhama, P. Fenici, in: Proc. of ISFNT XXX, 1997.